Available online at www.sciencedirect.com
SCIENCE DIRECT
Journal of Catalysis 241 (2006) 255–267
JOURNAL OF CATALYSIS
www.elsevier.com/locate/jcat

Role of Nb in rutile-type Cr/V/Sb/Nb mixed oxides, catalysts for propane ammoxidation to acrylonitrile

N. Ballarini [a], F. Cavani [a,*], M. Cimini [a], F. Trifirò [a], J.M.M. Millet [b], U. Cornaro [c], R. Catani [d]

[a] *Dip. Chimica Industriale e Materiali, V.le Risorgimento 4, 40136 Bologna, Italy* [1]
[b] *Institut de Recherches sur la Catalyse, CNRS, 2 av. A. Einstein, 69626 Villeurbanne cedex, France* [2]
[c] *EniTecnologie SpA, Via Maritano 26, 20097 San Donato Milanese MI, Italy*
[d] *Snamprogetti SpA, Viale De Gasperi 16, 20097 San Donato Milanese MI, Italy*

Received 12 January 2006; revised 28 March 2006; accepted 10 April 2006

Available online 6 June 2006

Abstract

Rutile-type Cr/V/Sb/Nb mixed oxides were prepared by coprecipitation from ethanolic solutions and calcination at 700 °C. They were then tested as catalysts for the gas-phase ammoxidation of propane. The addition of increasing amounts of Nb to the rutile Cr/V antimonate led to a considerable increase in the selectivity to acrylonitrile and to a lower selectivity to N_2 derived from ammonia overoxidation. But this effect was evident only when excess Sb was present with respect to the stoichiometric requirement for the formation of the rutile compound. Evidence was obtained for the development of rutile-type mixed Cr/V antimonate/niobate; this multicomponent rutile had a highly defective structure, with cationic vacancies in relation to excess Sb^{5+} with respect to the stoichiometric composition. The progressive increase of Nb concentration in this mixed oxide with increasing Nb loading led to a partial segregation of Sb oxide in the form of Sb_2O_4. The excess Sb in rutile provided the active sites for allylic ammoxidation on intermediate adsorbed propylene. The contemporaneous presence of Nb in the lattice improved the efficiency of these sites and was responsible for the better catalytic performance with respect to the Cr/V/Sb/O systems.

Keywords: Propane ammoxidation; Acrylonitrile; Rutile; Niobium oxide; Chromium; Vanadium; Antimony mixed oxides

1. Introduction

The synthesis of acrylonitrile is carried out by ammoxidation of propylene, but interest exists in developing a process that uses propane as the raw material, due to the lower cost of paraffin compared with olefin [1–3]. BP and Mitsubishi Chemical have developed processes for this reaction [4,5] and have announced the startup of semicommercial units or of pilot plants for the ammoxidation of propane. The catalysts claimed are based on either rutile-type metal antimonates (V/Sb/O, V/Al/Sn/Sb/O, Fe/Sb/O) [6–10] or mixed molybdates (Mo/V/Te(Sb)/Nb/O for the Mitsubishi catalyst) [11–14]. These catalysts are polyfunctional systems, with several components aimed at different roles in the multielectron complex transformation of the alkane, including propane activation and oxidehydrogenation, and the allylic ammoxidation of the unsaturated intermediate to acrylonitrile. With regard to this, the rutile-type structure has the necessary flexibility to accommodate various elements in its framework, with formation of a wide variety of solid solutions, and thus it represents the optimal system for the development of multicomponent catalysts.

Nb is claimed to play an important role in catalysts aimed at the oxidative transformation of hydrocarbons [15–17]. This is particularly true in Mo/V/Te(Sb)/Nb/O systems for propane oxidation to acrylic acid, in which the addition of Nb leads to increased selectivity to the desired product [18–21]. Niobium not only addresses the formation of specific crystalline structures, but also may exert a synergetic action on Te. In the Mo/V/Nb/O system, active and selective in the ethane oxidation to ethylene or to acetic acid [22–25], originally reported by Union Car-

* Corresponding author.
E-mail address: fabrizio.cavani@unibo.it (F. Cavani).
[1] INSTM, Research Unit of Bologna. A partner of Concorde CA and of Idecat NoE (6FP of the EC).
[2] A member of Concorde CA (6FP of the EC).

0021-9517/$ – see front matter
doi:10.1016/j.jcat.2006.04.016

bide [22] and then studied by others [23,24], Nb acts to enhance the intrinsic activity of Mo/V/O and to inhibit the combustion of ethane.

In the case of alkane ammoxidation, Nb is included in the formulation of Mitsubishi catalyst [11,13], but no specific role for this element in the reaction has yet been reported. The Nb/Sb/O system is used for the ammoxidation of ethane to acetonitrile [26], and the combination of Bi/Mo/O and alumina-supported Nb_2O_5 gives good performance in the ammoxidation of isobutane to methacrylonitrile [27]. Nb is one component of the V/Nb/Sb/O catalyst for propane ammoxidation developed by Nitto Chem Ind [28]. In recent work, Bañares et al. [29,30] found that when used as the support for V/Sb mixed oxide, Nb_2O_5 formed new phases by reaction with V and Sb under catalytic reaction conditions; these phases, of unclear nature, affected the catalytic performance in propane ammoxidation.

In previous work we studied the reactivity of Cr/Sb and of Cr/V/Sb mixed oxides [31–34] and found that rutile-like Cr antimonates were active and fairly selective for propane ammoxidation; additing V considerably improved catalyst activity, whereas the effect on selectivity to acrylonitrile was a function of the (Cr + V)/Sb ratio. Two main drawbacks of these systems were (i) the low selectivity to acrylonitrile, which at best was not more than 35% at total conversion of oxygen (the limiting reactant under propane-rich conditions), and (ii) the high activity in ammonia oxidation to molecular nitrogen.

In the present work, we analyze the effect of Nb addition on catalytic performance of rutile-type Cr/V/Sb/O systems.

2. Experimental

Catalysts were prepared with the coprecipitation technique, developed for the preparation of rutile SnO_2-based systems claimed by Rhodia [7]. The preparation involves the dissolution of $Cr(NO_3)_3{\cdot}6H_2O$, $VO(acac)_2$, $SbCl_5$, and $NbCl_5$ in absolute ethanol, followed by dropping the solution into a buffered aqueous solution maintained at pH 7. The precipitate thus obtained is separated from the supernatant liquid by centrifugation and filtration. The solid is then dried at 120 °C and calcined in air at 700 °C for 3 h at a heating rate of 1 °C/min.

The X-ray diffraction (XRD) patterns of the catalysts were obtained with Ni-filtered Cu$K\alpha$ radiation ($\lambda = 1.54178$ Å) on a Philips X'Pert vertical diffractometer equipped with a pulse height analyser and a secondary curved graphite crystal monochromator. Laser-Raman spectra were obtained using a Renishaw 1000 instrument; the samples were excited with the 514-nm Ar line. Specific surface areas were measured by the BET method with nitrogen adsorption (Thermo Instruments).

Sb L_1-edge XANES spectra were collected at the ID26 station (ESRF, Grenoble, France) using a pair of Si(220) crystals monochromated for energy selection. The electron energy was 6.0 GeV, and the ring current varied between 150 and 200 mA. Harmonic rejection was performed using two silicon mirrors at 2.8 and 4.3 mrad. Three spectra were recorded for each sample in the fluorescence mode during a 63-s scan from 4.66 to 5.60 keV in steps of 0.3 eV with a detector (Si diode) mounted at 90° with respect to the incident beam. To compare the different Sb L_1-edge XANES spectra, the absorption background was first carried out using a linear law over the entire range, and then the spectra were normalized in the middle of the first EXAFS oscillation, at ca. 50 eV above the absorption edge. $SbPO_4$ (4702.5 eV for Sb^{3+}) and $FeSbO_4$ (4707.5 eV for Sb^{5+}) reference spectra were taken as model data for Sb^{3+} and Sb^{5+}, respectively [35]. After normalization and background subtraction, the spectra were fitted using the PEAKFIT program.

XPS measurements were performed with a VG ESCALAB 200 R. Charging of the samples was corrected by setting the binding energy of adventitious carbon (C_{1s}) at 284.5 eV. Deconvolution of the $Sb_{3d_{3/2}}$ peak was accomplished using a Voigt function. Because of its low intensity and overlapping by satellite peak of O_{1s} no attempt to deconvolute the $V_{2p_{3/2}}$ peak was made. The experimental precision on the quantitative measurements was considered to be around 10%.

Catalytic tests were carried out in a laboratory stainless steel fixed-bed reactor operating at atmospheric pressure. A 1.8-g sample of catalyst, with particles ranging in size from 0.42 to 0.55 mm, was loaded. The following reaction conditions were used: feed composition, 25 mol% propane, 10% ammonia, 20% oxygen, remainder helium; residence time 2.0 s. The reactor outlet temperature was maintained at 170 °C. On-line sampling of a volume of either the feedstock or effluents was obtained by means of three heated valves. Three different columns were used for product identification: a Hay-sep T columns (thermal conductivity detector [TCD]) for separation of CO_2, NH_3, $C_3H_8 + C_3H_6$, H_2O, HCN, acrolein, acetonitrile, and acrylonitrile and a MS-5A column (TCD) for separation of O_2, N_2, and CO. A Hay-sep T column was also used as a filter to avoid contamination of MS-5A by CO_2. The third column was a packed one filled with Poropak QS (flame ionization detector) used to separate propane from propylene.

3. Results

3.1. Characterization of Cr/V/Sb/Nb/O samples: Specific surface areas

Table 1 reports the composition of catalysts prepared (atomic ratios between components), along with their corresponding specific surface areas. The samples prepared are grouped into four different series, in which either the amount of Sb (series with atomic ratios between components equal to Cr/V/Sb/Nb 1/0.2/x/1 and 1/1/x/1) or the amount of Nb (series with atomic ratios between components equal to Cr/V/Sb/Nb 1/0.2/1/x and 1/0.2/5/x) has been varied. In the latter case, the amount of Sb has been kept either close to the Cr + V sum (Cr/V/Sb/Nb 1/0.2/1/x) or in large excess with respect to it (Cr/V/Sb/Nb 1/0.2/5/x). In all cases, the compositions have been referred to the atomic amount of Cr, fixed to 1.

Concerning the specific surface areas, the following effects were observed:

(a) An increase in Sb content led to an increase in surface area, which may be linked to the decreased crystallinity as inferred from XRD patterns (see below).

Table 1
Composition of catalysts, and specific surface area

Cr/V/Sb/Nb atomic ratios	Specific surface area (m^2/g)
Series Cr/V/**Sb**/Nb 1/1/x/1	
1/1/0/1	11
1/1/1/1	24
1/1/3/1	31
1/1/5/1	32
Series Cr/V/**Sb**/Nb 1/0.2/x/1	
1/0.2/0/1	20
1/0.2/1/1	34
1/0.2/3/1	80
1/0.2/5/1	87
Series Cr/V/Sb/**Nb** 1/0.2/1/x	
1/0.3/1.1/0	59
1/0.2/1/0.2	51
1/0.2/1/1	34
Series Cr/V/Sb/**Nb** 1/0.2/5/x	
1/0.2/5/0	51
1/0.2/5/0.2	83
1/0.2/5/1	87
1/0.2/5/1.7	88

(b) A decreased V content with a constant atomic ratio between the other components led to higher surface area values; also in this case, this could correspond to a lower crystallinity of the samples.
(c) The effect of Nb on surface area was a function of the Sb content in samples; in the case of catalysts of composition Cr/V/Sb/Nb 1/0.2/1/x, which maintained good crystallinity along with the variation of the Nb content, a decrease in surface area was observed with increasing Nb content. The opposite was true for samples of composition Cr/V/Sb/Nb 1/0.2/5/x, which exhibited lower crystallinity than those containing less Sb.

3.2. Characterization of Cr/V/Sb/Nb/O samples: The effect of varying Sb content

Fig. 1 shows the XRD patterns of samples belonging to the series Cr/V/Sb/Nb 1/1/x/1 and 1/0.2/x/1. In Cr/V/Sb/Nb 1/1/0/1 (the Sb-free catalyst), the main reflections were almost coincident with those of the stoichiometric tetragonal rutile-type mixed oxide $CrVNbO_6$ [36] containing V with a 4+ oxidation state; in contrast, the peak positions differed from those of stoichiometric $CrNbO_4$ and of $VNbO_4$ [37]. For instance, the (2, 1, 1) reflection is positioned at 2θ 54.05° for $CrVNbO_6$ (JCPDS file 36-0788), at 2θ 53.55° for $CrNbO_4$ (JCPDS file 34-0366), at 2θ 53.0° for $VNbO_4$ [37], compared with 2θ 53.9° for Cr/V/Sb/Nb 1/1/0/1. However, weak reflections attributable to V_2O_5 (JCPDS file 41-1426) indicate that either the formation of the mixed oxide was not quantitative or the mixed oxide formed indeed had a slightly different, V-deficient stoichiometry (e.g., $Cr_{1+x}V_{1-2x}Nb_{1+x}O_6$). For Cr/V/Sb/Nb 1/1/1/1, the most intense reflections were once again attributable to the tetragonal, rutile-type compound, with additional weak reflections corresponding to V_2O_5 and VNb_9O_{25} (JCPDS file 18-1447). The presence of an increasing amount of Sb in the 1/1/x/1 series led to an evident decrease in crystallinity of the rutile-type mixed oxide with a shift of reflections toward lower 2θ values, indicating increases in cell volume presumably linked to the replacement of cations in the structure with bigger ones.

Analogous effects were observed when the amount of Sb was increased within the series Cr/V/Sb/Nb 1/0.2/x/1; the shift toward lower 2θ values was evident, as was the decrease of crystallinity. The main difference with patterns of samples of composition Cr/V/Sb/Nb 1/1/x/1 appeared to be the absence of the weak reflections relative to V_2O_5; this was clearly due to the lower V oxide content.

It is noteworthy that the cation of octahedral Nb^{5+} (0.64 Å) is larger than that of Sb^{5+} (0.60 Å); this implies a smaller volume of the tetragonal crystallographic cell for rutile $CrSbO_4$ than for rutile $CrNbO_4$ (64.978 $Å^3$ for $CrNbO_4$ vs 64.308 $Å^3$ for $CrSbO_4$). Therefore, the shift in reflections observed with increasing Sb cannot be explained by the replacement of Nb^{5+} with smaller Sb^{5+}. One possible explanation for these two phenomena (i.e., the increased unit cell volume and the decreased crystallinity) is the formation of a nonstoichiometric rutile compound, in which Sb^{5+} substitutes smaller cations (e.g., V^{4+}, the cation size of which is 0.58 Å) or develops interstitial solid solutions. In both cases, the presence of excess positive charges might be compensated for by either the generation of cationic vacancies (see the discussion on Raman spectra, Fig. 2) or the reduction of an equivalent amount of V^{4+} to V^{3+}. Another possible explanation is the incorporation of excess Sb in the form of Sb^{3+} cation (0.76 Å), into those positions normally occupied by Cr^{3+} (0.69 Å) or V. However, XANES results (see below) will not support this hypothesis; the large size of Sb^{3+} compared with the other cations also makes its introduction inside the rutile lattice unlikely.

Raman spectra of samples are shown in Fig. 2. The spectra of Cr/V/Sb/Nb 1/1/0/1 and 1/0.2/0/1 (the Sb-free samples) showed an intense broad band at Raman shift 800 cm^{-1}, corresponding to no band in either chromium oxide or any niobium or vanadium oxide, and a less intense band at 920 cm^{-1} that was more evident in Cr/V/Sb/Nb 1/1/0/1. The spectrum of Cr/V/Sb/Nb 1/0.2/0/1 was the same as that of tetragonal $CrNbO_4$ [37], whereas rutile $CrSbO_4$ had an intense band at 760 cm^{-1} and a less intense one at 670 cm^{-1} [31]; moreover, the spectrum of Cr/V/Sb/Nb 1/0.2/0/1 was different from that of any V/Nb mixed oxide, including rutile-type $VNbO_4$ [37,38].

For Cr/V/Sb/Nb 1/1/x/1, the addition of Sb modified the spectrum with respect to the Sb-free catalyst. In Cr/V/Sb/Nb 1/1/1/1, besides bands attributable to V_2O_5 (the presence of which had also been identified by XRD; Fig. 1), bands relative to rutile vibrations were weaker than those in Cr/V/Sb/Nb 1/1/0/1, although falling at the same wavenumbers. The spectra of samples with excess Sb ($x = 3$ and 5) were considerably different; a broad band attributable to Sb_6O_{13} appeared in the 450–480 cm^{-1} range, whereas bands attributable to V_2O_5 disappeared. The band at 900–920 cm^{-1} was very intense, whereas that at 800 cm^{-1} was no longer present (or at

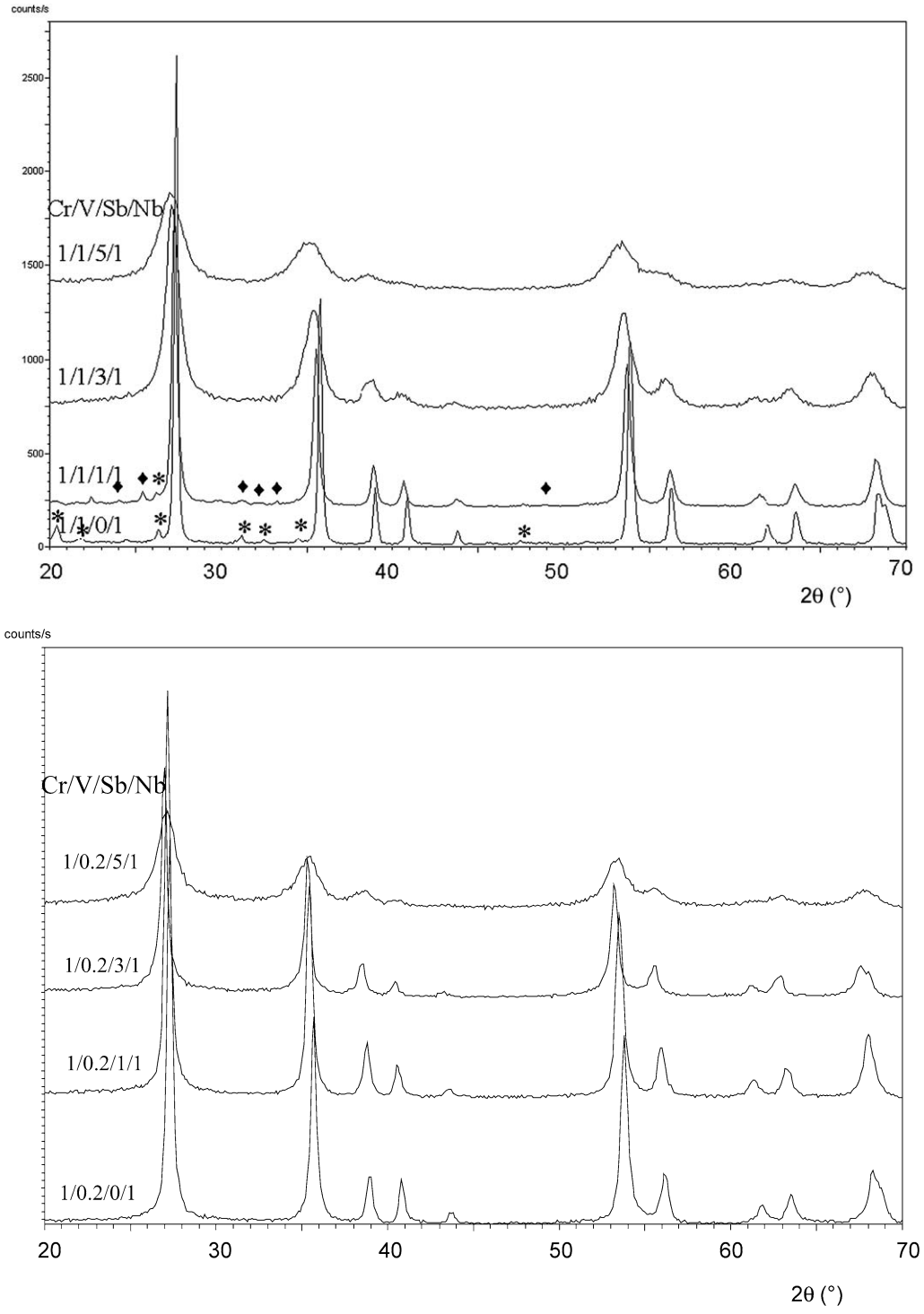

Fig. 1. X-Ray diffraction pattern of samples Cr/V/Sb/Nb 1/1/x/1 and 1/0.2/x/1, calcined at 700 °C. (*) V_2O_5. (◆) VNb_9O_{25}.

least was overlapped by the former). Bands at 740–750 and 670 cm^{-1} were also observed in almost stoichiometric rutile-type $CrSbO_4$ [31].

Quite similar spectra were recorded in the case of Cr/V/Sb/O samples, when the (Cr + V) atomic amount was much lower than the Sb one [34] (e.g., in Cr/V/Sb 1/1/5); bands were observed at 990, 890, 740, 660, 575, and 465 cm^{-1} that clearly correspond with bands observed in the spectrum of Cr/V/Sb/Nb 1/1/5/1. In the former case, evidence was obtained for the formation of a mixed V^{3+}/Cr^{3+} antimonate.

Raman spectrum of Cr/V/Sb/Nb 1/0.2/1/1 was similar to that of Cr/V/Sb/Nb 1/1/0/1, while the spectrum of Cr/V/Sb/Nb 1/0.2/3/1 resembled that of Cr/V/Sb/Nb 1/1/5/1. Specifically, bands at 660–670, 740–750, and 900–920 cm^{-1}, which were very weak in the spectra of samples with $x = 0$ and 1, became evident in the sample with $x = 3$. Therefore, for these

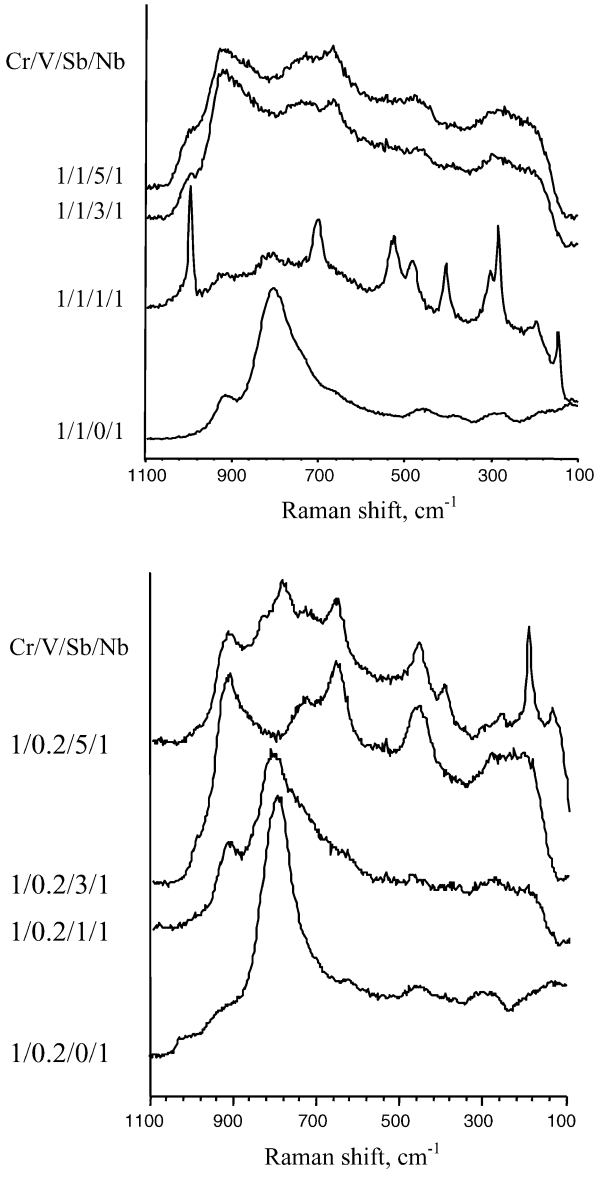

Fig. 2. Raman spectra of samples Cr/V/Sb/Nb 1/1/x/1 and 1/0.2/x/1, calcined at 700 °C.

samples many analogies exist with catalysts belonging to the Cr/V/Sb/Nb 1/1/x/1 series. More relevant differences were observed between spectra of Cr/V/Sb/Nb 1/0.2/5/1 and 1/1/5/1; in the former case, besides the band at 460–465 cm^{-1} relative to Sb_6O_{13}, others attributable to α-Sb_2O_4 were present at 195 and 400 cm^{-1} that were not observed in Cr/V/Sb/Nb 1/1/5/1. Moreover, two bands at 790 and 830 cm^{-1} were clearly evident in Cr/V/Sb/Nb 1/0.2/5/1; the latter are discussed in reference to spectra of Cr/V/Sb/Nb 1/0.2/5/x (see below). They seem to derive from a progressive modification of the main band of $CrNbO_4$ at 800 cm^{-1}.

From the literature [39], the spectrum of nonstoichiometric rutile V/Sb/O of composition $V_{0.92}Sb_{0.92}O_4$ is badly resolved and shows a broad band at 880 cm^{-1}, assigned to vibration modes involving 2-coordinated O species. In the absence of cationic vacancies, when only 3-coordinated O species are present, the Raman spectrum has only diffuse features, with a very broad band centered at approximately 720 cm^{-1}.

3.3. Characterization of Cr/V/Sb/Nb/O samples: The effect of varying Nb content

The XRD patterns and Raman spectra of Cr/V/Sb/Nb 1/0.2/5/x and 1/0.2/1/x are presented in Figs. 3 and 4, respectively. Samples with higher amounts of Sb were much less crystalline than those of the series Cr/V/Sb/Nb 1/0.2/1/x, in agreement with patterns reported in Fig. 1. Weak reflections attributable to Sb_6O_{13}, in the pattern of the Nb-free sample Cr/V/Sb/Nb 1/0.2/5/0, disappeared in the Nb-containing samples; apart from this, the only reflections relative to the rutile-type structure were evident for all samples of both series. In this case, the increase in Nb content led to a very small variation in peak position.

Raman spectra provided further information. The spectrum of Cr/V/Sb/Nb 1/0.3/1.1/0 (a Nb-free catalyst) was very similar to that of $CrSbO_4$ [31], with two main bands at 760 and 670 cm^{-1}. The addition of increasing amounts of Nb in the series Cr/V/Sb/Nb 1/0.2/1/x led to the displacement of the main bands toward higher wavenumbers; the spectrum of Cr/V/Sb/Nb 1/0.2/1/1 shows two main bands at 910–920 and 800 cm^{-1}.

In the case of Sb-richer samples, the increasing amount of Nb led to the following:

(a) Increased intensity of bands relative to α-Sb_2O_4; this may indicate that Nb^{5+} replaced Sb in the rutile-type mixed oxide, and, consequently, excess antimony formed Sb_2O_4.
(b) Increased intensity of bands at 830 and 790 cm^{-1} (already mentioned in reference to Cr/V/Sb/Nb 1/0.2/5/1), which are not related to any Nb or Sb oxides. Attributing these bands is difficult; $VSbO_4$ [10] and $CrNbO_4$ [37] each had a broad band falling in this range, whereas orthorhombic $VNbO_5$ was characterized by a band centered at around 730–750 cm^{-1}. α-Sb_2O_4 itself had bands at 820, 750, and 710 cm^{-1}, but these were much weaker than the most intense ones at 190–200 and 400 cm^{-1} [40]. The formation of $SbNbO_4$, a mixed-oxide isostructural with α-Sb_2O_4, can be excluded; in fact, this compound yielded broad bands at 850, 690, and 620 cm^{-1} [29,30].
(c) Increased intensity of the band at 900–920 cm^{-1}.

Samples belonging to the series Cr/V/Sb/Nb 1/0.2/5/x were characterized by means of XANES spectroscopy at the Sb L_1 edge (Fig. 5) and XPS (Table 2). In the XANES spectra, the deconvolution of the Sb L_1-edge peak allowed us to determine the relative amounts of Sb^{3+} (4703.2–4703.5 eV) and of Sb^{5+} (4707.4–4707.5 eV). Sb was found to be present mainly as Sb^{5+}, with the relative amount of Sb^{3+} species close to 5% in all cases. More specifically, the $Sb^{3+}/(Sb^{3+} + Sb^{5+})$ was equal to 6% when $x = 0.2$, to 5% when $x = 1$, and to 4% when $x = 1.7$.

The low amount of Sb^{3+} despite the large excess of Sb indicates that the major fraction of this element was present

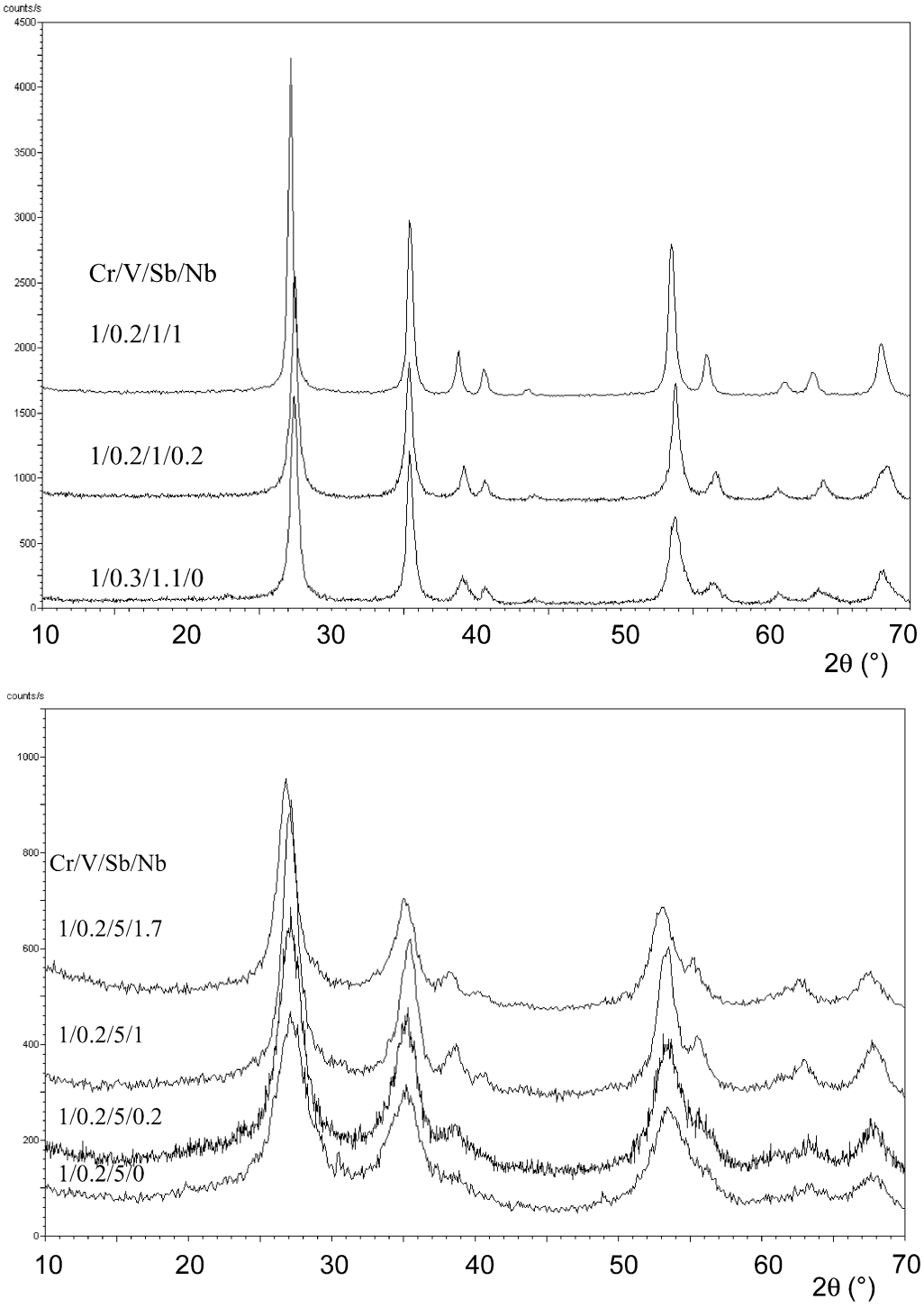

Fig. 3. X-Ray diffraction pattern of samples Cr/V/Sb/Nb 1/0.2/5/x and 1/0.2/1/x, calcined at 700 °C.

in the rutile framework as Sb^{5+}, rather than dispersed over the rutile surface in the form of Sb^{3+}-containing Sb oxides, that is, Sb_6O_{13} and/or Sb_2O_4. This agrees with the indications in previous work on the formation of Sb^{5+}-enriched rutile-type solid solutions in Cr/(V)/Sb mixed oxides [31,34]. This excess Sb^{5+} generated a corresponding amount of cationic vacancies and thus was responsible for the low crystallinity of these samples. On the other hand, positive effects were the high specific surface areas (much higher than those of V/Sb/O samples calcined under the same conditions) and the development of surface sites specific for allylic ammoxidation.

Table 2 reports the main results of XPS measurements. The table also compares the atomic ratios between elements and Sb for the bulk, as inferred from the catalyst composition, and for the surface, as determined from XPS data. It also reports the fraction of Sb^{3+} as calculated from the relative intensity ratio of peaks obtained from the deconvolution of the broad $Sb_{3d_{3/2}}$

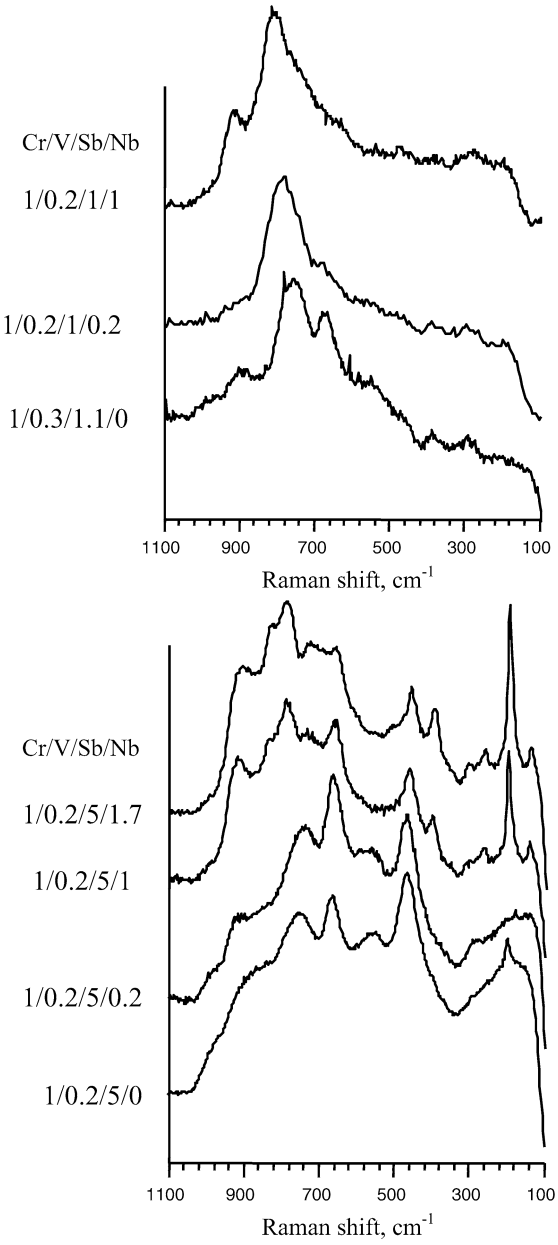

Fig. 4. Raman spectra of samples Cr/V/Sb/Nb 1/0.2/5/x and 1/0.2/1/x, calcined at 700 °C.

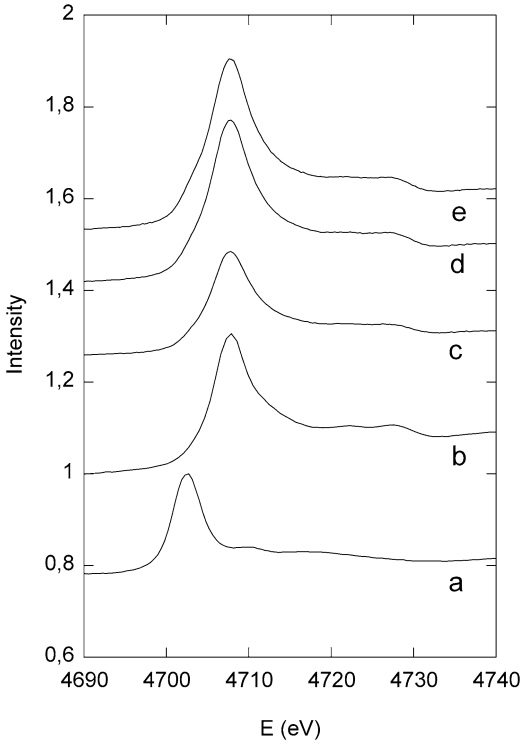

Fig. 5. XANES spectra of samples Cr/V/Sb/Nb 1/0.2/5/x, calcined at 700 °C. (a) Reference $SbPO_4$; (b) reference $FeSbO_4$; (c) $x = 0.2$; (d) $x = 1.0$; (e) $x = 1.7$.

Table 2
Results of XPS characterization of samples Cr/V/Sb/Nb 1/0.2/5/0.2, 1/0.2/5/1 and 1/0.2/5/1.7

Catalyst Cr/V/Sb/Nb	Element M	Binding energy (eV)	M/Sb atomic ratio		$Sb^{3+}/(Sb^{3+}+Sb^{5+})$
			Bulk	XPS	
1/0.2/5/0.2	$Cr_{2p_{3/2}}$	577.6	0.2	0.10	
	$Sb_{3d_{3/2}}$	540.6, 539.8	–	–	0.04
	$O_{1s_{5/2}}$	530.8		2.00	
	$Nb_{3d_{5/2}}$	207.3	0.04	0.02	
	$V_{2p_{3/2}}$	517.8	0.04	0.06	
1/0.2/5/1	$Cr_{2p_{3/2}}$	577.4	0.2	0.11	
	$Sb_{3d_{3/2}}$	540.6, 539.8	–	–	0.12
	$O_{1s_{5/2}}$	530.7		2.51	
	$Nb_{3d_{5/2}}$	207.4	0.2	0.11	
	$V_{2p_{3/2}}$	517.8	0.04	0.09	
1/0.2/5/1.7	$Cr_{2p_{3/2}}$	578.1	0.2	0.12	
	$Sb_{3d_{3/2}}$	540.6, 539.8	–	–	0.13
	$O_{1s_{5/2}}$	530.5		2.29	
	$Nb_{3d_{5/2}}$	207.5	0.34	0.22	
	$V_{2p_{3/2}}$	517.7	0.04	0.10	

peak into the two components at 540.6 and 539.8 eV. It is clear that this type of operation has a great degree of uncertainty, however. The small peak relative to $V_{2p_{3/2}}$ did not allow such a deconvolution, also because it was superimposed to a satellite peak of O_{1s}; therefore, attributing it to a specific oxidation state for V was not possible. However, the BE was lower than that typically observed for V^{5+}, and therefore the average oxidation state for V was likely lower than 5+. The Nb energy corresponded to Nb^{5+}; the Cr energy, to Cr^{3+}.

The Cr/Sb and V/Sb surface ratios were slightly lower and higher than the corresponding bulk surface ratio, respectively, suggesting either a slight surface enrichment of V or intracrystalline gradients of each one of the two elements in the rutile lattice. In the case of V, moreover, the surface ratio increased with increasing Nb content, suggesting the possible formation of V/Nb mixed oxides spread at the surface of the rutile phase. It is worth mentioning, however, that due to the very low amount of V and the corresponding low intensity of the V_{2p} peak, any consideration regarding this element as inferred from XPS spectra was not fully certain.

There was an excess of Sb with respect to Cr and Nb that was larger than the bulk one; this indicates a surface enrichment of

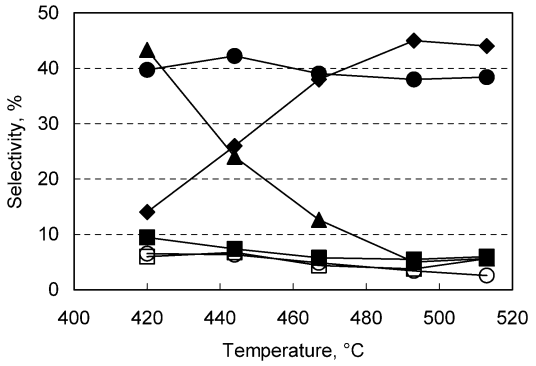

Fig. 6. Selectivity to acrylonitrile (◆), to cyanhydric acid (▲), to propylene (■), to carbon dioxide (●), to carbon monoxide (□) and to acetonitrile (○) as functions of the reaction temperature. Catalyst: Cr/V/Sb/Nb 1/0.2/5/1.7. Reaction conditions: feed composition 25 mol% propane, 10% ammonia, 20% oxygen, remainder He; residence time 2.0 s.

Sb that might correspond to the spreading of Sb oxide over the rutile surface. However, it is worth mentioning that the large amount of Sb in samples should lead to much lower M/Sb surface ratios than the experimental ones, if all Sb in excess with respect to the stoichiometric requirement for rutile formation segregated at the surface in the form of Sb oxide. This supports the view that indeed the rutile phase was nonstoichiometric and contained excess Sb^{5+} in the bulk with respect to the stoichiometric formula.

An increase in Nb content led to an increase in the Nb/Sb surface ratio (approximately half of the bulk one for all samples), but this ratio remained proportional to the Nb content. This indicates that there was no preferential segregation of Nb oxide at the surface of rutile, confirming the hypothesis of dissolution of Nb^{5+} in the rutile lattice. Moreover, a slight increase in the relative amount of surface Sb^{3+} (while the same amount, as calculated from XANES spectroscopic data, apparently remained constant) supports the view that the replacement of Nb^{5+} for Sb in the rutile led to the segregation of Sb_2O_4 at the surface.

3.4. Reactivity of Cr/V/Sb/Nb/O catalysts in propane ammoxidation

Fig. 6 plots the effect of temperature on the selectivity to the different products for Cr/V/Sb/Nb 1/0.2/5/1.7, which gave the highest selectivity to acrylonitrile among all of the Nb-containing catalysts described in the present work. Fig. 9 shows the corresponding propane conversion and compares it with that of the other samples in the Cr/V/Sb/Nb 1/0.2/5/*x* series. Increasing temperature had a remarkable effect on the selectivity to acrylonitrile, which increased mainly at the expense of cyanhydric acid; the latter was the prevailing product at low reaction temperatures. The relative amounts of the other byproducts (i.e., carbon dioxide, carbon monoxide, propylene, and acetonitrile) were not substantially affected by temperature.

Fig. 7 compares the catalytic performance of samples of composition Cr/V/Sb/Nb 1/0.2/*x*/1. The figure plots the conversion of propane, selectivity to acrylonitrile, and selectivity to molecular nitrogen, calculated with respect to ammonia converted, as functions of the reaction temperature; it also reports the selectivity to the products at 405–425 °C. The catalyst without Sb (Cr/V/Sb/Nb 1/0.2/0/1) was extremely active (with total conversion of oxygen reached already at 390–400 °C), but was

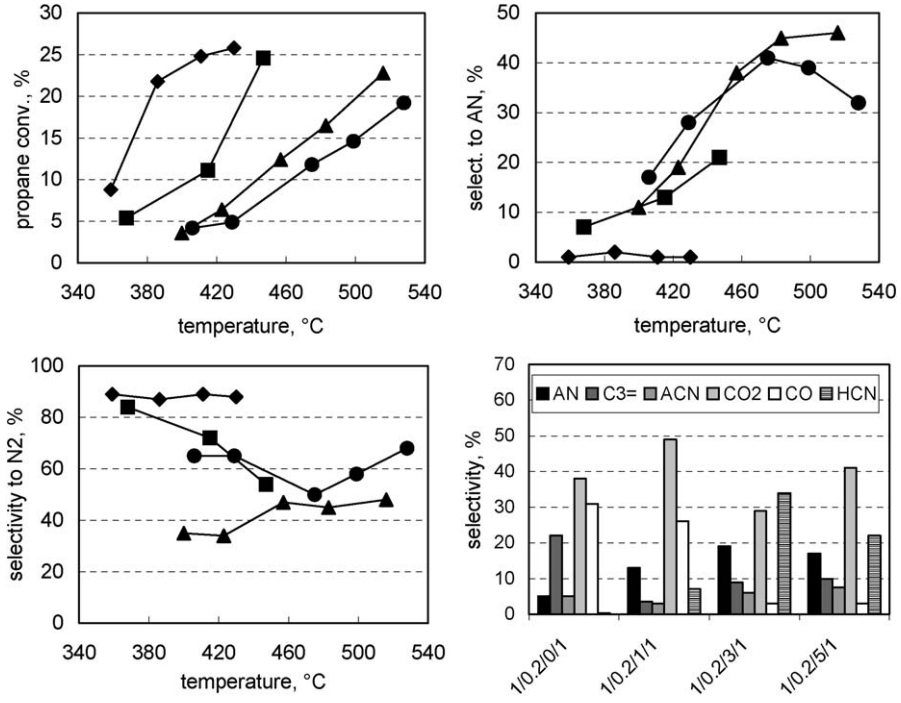

Fig. 7. Effect of temperature on propane conversion (top left), on selectivity to acrylonitrile (top right) and on selectivity to N_2 from ammonia combustion (bottom left). Distribution of products at ≈405–425 °C (bottom right): AN acrylonitrile; C3= propylene; ACN acetonitrile; CO2 carbon dioxide; CO carbon monoxide; HCN cyanhydric acid. Catalysts Cr/V/Sb/Nb 1/0.2/*x*/1: 1/0.2/0/1 (◆), 1/0.2/1/1 (■), 1/0.2/3/1 (▲), and 1/0.2/5/1 (●). Reaction conditions as in Fig. 6.

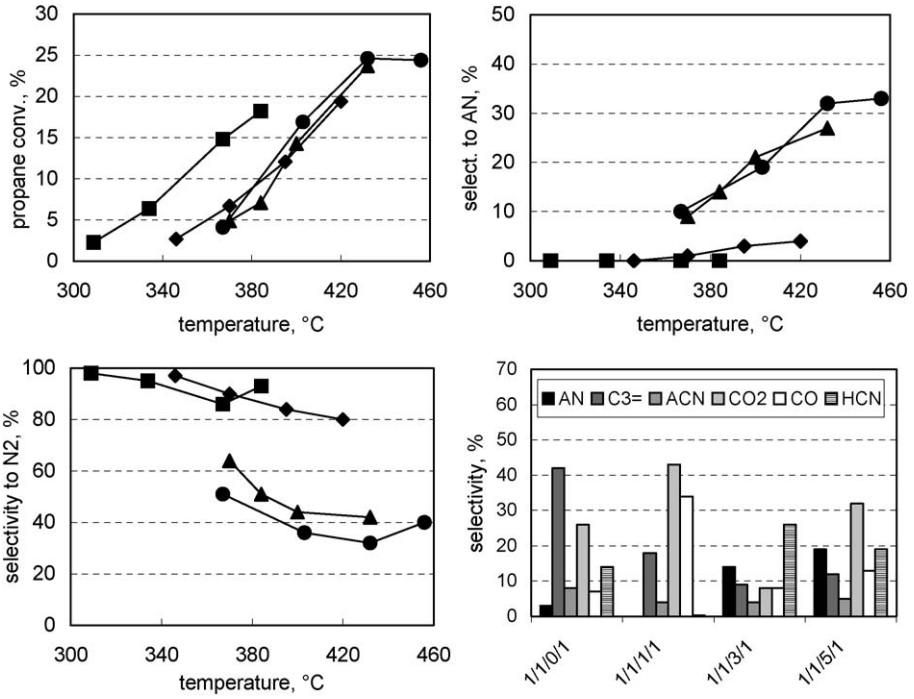

Fig. 8. Effect of temperature on propane conversion (top left), on selectivity to acrylonitrile (top right) and on selectivity to N_2 from ammonia combustion (bottom left). Distribution of products at ≈385–405 °C (bottom right): AN acrylonitrile; C3= propylene; ACN acetonitrile; CO2 carbon dioxide; CO carbon monoxide; HCN cyanhydric acid. Catalysts Cr/V/Sb/Nb 1/1/x/1: 1/1/0/1 (◆), 1/1/1/1 (■), 1/1/3/1 (▲), and 1/1/5/1 (●). Reaction conditions as in Fig. 6.

nonselective to acrylonitrile (with most ammonia oxidized to N_2); the main products were propylene, CO, and CO_2. This catalytic behavior was similar to that of the Cr/V/Sb 1/x/1 catalysts, which in general were very active and poorly selective to acrylonitrile and in which the increasing content of V led to a higher selectivity to propylene [33,34].

The addition of increasing amounts of Sb caused a decrease in activity. The selectivity to acrylonitrile and HCN increased, with a correspondingly lower selectivity to propylene and CO; the degree of ammonia oxidized to N_2 decreased. The catalyst with the greatest amount of Sb (Cr/V/Sb/Nb 1/0.2/5/1) had a maximum selectivity to acrylonitrile, which was achieved well below the temperature at which total conversion of oxygen was reached.

For the catalysts with higher V content (series Cr/V/Sb/Nb 1/1/x/1; Fig. 8), all samples were very active. Cr/V/Sb/Nb 1/1/1/1 was more active than the corresponding Sb-free sample (Cr/V/Sb/Nb 1/1/0/1), but a further increase in Sb content ($x = 3$ and 5) led to decreased activity. Moreover, the two former compounds were unselective to acrylonitrile, as was the Nb-free catalyst Cr/V/Sb 1/1/1 [33]. They had comparable activity in ammonia conversion (not shown), which was almost completely converted to N_2, but had differing product distributions. Cr/V/Sb/Nb 1/1/0/1 was more selective to propylene and HCN, whereas Cr/V/Sb/Nb 1/1/1/1 was more selective to CO_2 and CO. Excess Sb led to an increased selectivity to acrylonitrile and cyanhydric acid at the expense of selectivity to propylene and carbon oxides.

These data indicate that $CrVNbO_6$ (Cr/V/Sb/Nb 1/1/0/1) and $CrVNbSbO_8$ (Cr/V/Sb/Nb 1/1/1/1) are active catalysts for propane ammoxidation but are quite unselective to acrylonitrile; prevailing products were either propylene or carbon oxides, depending on catalyst composition. The same applies for Cr/V/Sb/Nb/O catalysts with a (Cr + V)/(Sb + Nb) atomic ratio close to 1. Catalysts in which this ratio was largely < 1, due to the presence of excess Sb, were instead selective to acrylonitrile.

The relevant formation of N_2 and the very low selectivity to products of partial (amm)oxidation observed for Cr/V/Sb/Nb 1/1/0/1 and 1/1/1/1 can be related to the presence of crystalline V_2O_5, as evident from both XRD patterns (Fig. 1) and Raman spectra (Fig. 2). It is noteworthy that besides these two catalysts, other samples giving high selectivity to N_2 were Cr/V/Sb/Nb 1/0.2/0/1 (Fig. 7), 1/0.3/1.1/0, and 1/0.2/1/0.2 (Fig. 10); these were the catalysts in which the presence of V_2O_5, although detected in very small amounts, was identified by means of Raman spectroscopy; see, for example, the very weak band at ≈1000 cm^{-1} in the spectrum of Cr/V/Sb/Nb 1/0.2/0/1 (Fig. 2) or in that of 1/0.3/1.1/0 (Fig. 4).

Fig. 9 compares the effect of Nb in catalysts Cr/V/Sb/Nb 1/0.2/5/x. Increasing values of x led to a slight increase in propane and ammonia conversion; in general, these catalysts were less active than those with lower Sb content. The main effect, however, was on the selectivity to acrylonitrile, which was 10–15% higher in the samples with the highest Nb content. The selectivity to carbon dioxide was correspondingly lower. Other byproducts (e.g., propylene, carbon monoxide, cyanhydric acid, and acetonitrile) formed with selectivity <10%. One important characteristic of Nb-containing catalysts was the low extent of ammonia combustion to molecular nitrogen; whereas Cr/V/Sb/Nb 1/0.2/5/0 and 1/0.2/5/0.2 converted most ammonia to N_2, in Cr/V/Sb/Nb

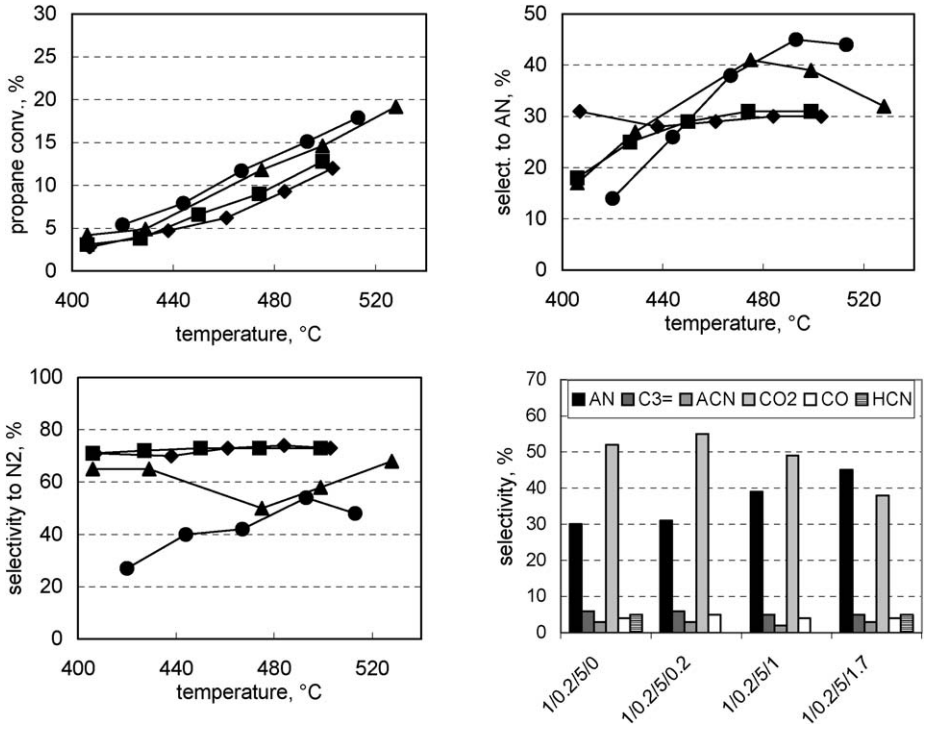

Fig. 9. Effect of temperature on propane conversion (top left), on selectivity to acrylonitrile (top right) and on selectivity to N_2 from ammonia combustion (bottom left). Distribution of products at ≈493–503 °C (bottom right): AN acrylonitrile; C3= propylene; ACN acetonitrile; CO2 carbon dioxide; CO carbon monoxide; HCN cyanhydric acid. Catalysts Cr/V/Sb/Nb 1/0.2/5/x: 1/0.2/5/0 (◆), 1/0.2/5/0.2 (■), 1/0.2/5/1 (▲), and 1/0.2/5/1.7 (●). Reaction conditions as in Fig. 6.

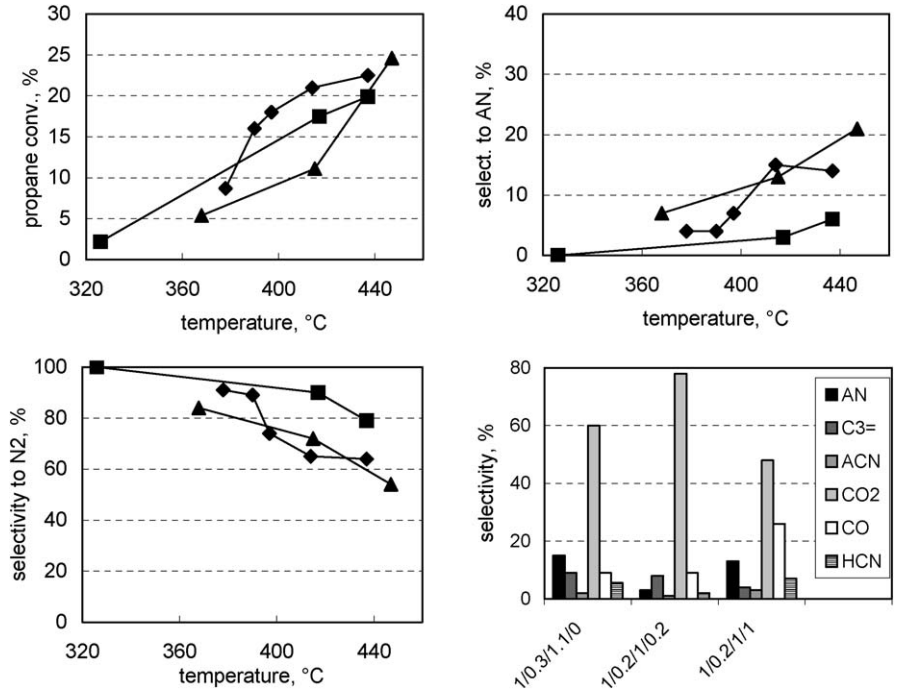

Fig. 10. Effect of temperature on propane conversion (top left), on selectivity to acrylonitrile (top right) and on selectivity to N_2 from ammonia combustion (bottom left). Distribution of products at ≈415–417 °C (bottom right): AN acrylonitrile; C3= propylene; ACN acetonitrile; CO2 carbon dioxide; CO carbon monoxide; HCN cyanhydric acid. Catalysts Cr/V/Sb/Nb 1/0.2/1/x: 1/0.3/1.1/0 (◆), 1/0.2/1/0.2 (■), and 1/0.2/1/1 (▲). Reaction conditions as in Fig. 6.

1/0.2/5/1 and 1/0.2/5/1.7, the fraction of ammonia burnt was ⩽65%.

The same positive effect due to Nb addition was not obtained in samples with low Sb content; this is shown in Fig. 10 for the series Cr/V/Sb/Nb 1/0.2/1/x. A low content of Sb led to very active catalysts, with the total conversion of oxygen reached already at 420–440 °C. Increasing amounts of Nb caused a slight decrease in activity. Furthermore, cata-

lysts were poorly selective to acrylonitrile (maximum selectivity of 20%), due to the relevant formation of CO_2. The addition of Nb did not lead to noticeable changes in product distributions, apart from an increase in carbon monoxide selectivity, with a corresponding decrease in carbon dioxide. No clear effects were observed on the selectivity to N_2. Therefore, obtaining a selectivity improvement effect from the addition of Nb required an excess of Sb with respect to the amount required for the development of the rutile-type compound.

4. Discussion

In previous work, it was found that in Cr/V/Sb systems the atomic ratio (Cr + V)/Sb was the main compositional parameter affecting the nature of these crystalline compounds [33,34]. When almost equiatomic ratios were used (e.g., in Cr/V/Sb 1/1/1), the corresponding XRD pattern showed the presence of a well-crystallized rutile-type compound. Because the Rietveld analysis of the diffraction profile indicated that an almost equiatomic composition of the rutile compound was most likely (when the Cr/Sb ratio was fixed to 1), formation of the compound $CrVSbO_6$ was hypothesized [33], which in practice corresponds to an equimolar solid solution between $CrSbO_4$ and VO_2 (both characterized by the rutile-type structure). In Cr/V/Sb/O samples with atomic ratios of Cr/V/Sb $1/x/1$, the general formula $Cr_1V_xSb_1O_{4+2x}$ was extrapolated. Alternatively, the replacement of Cr^{3+} with V^{4+} would generate an excess of positive charges, compensated for by either the formation of cationic vacancies or the reduction of Sb; indeed, very weak bands at 910 cm^{-1} developed, indicating the existence of cationic vacancies [33]. However, the absence of Cr oxide suggested that nondefective structures, with composition ranging from $CrSbO_4$ to $CrVSbO_6$, formed, rather than substitutional oxides with replacement of Cr^{3+} by either V^{3+} or V^{4+}. In addition, the replacement of Sb^{5+} with V was excluded, due to the absence of any Sb oxide in samples with increased V content. In these catalysts, V was present mainly as V^{4+}, and samples were extremely active in propane ammoxidation but poorly selective to acrylonitrile, leading to the prevailing formation of propylene and carbon oxides.

When instead samples were prepared with an atomic ratio (Cr + V)/Sb < 1, V was present mainly in the rutile mixed oxide as a V^{3+} species [33,34]. The main peculiarity of these Cr-based antimonates was found to be the ability to host excess Sb in the structure [31], thereby developing nonstoichiometric compounds, especially in samples with lower V content. Another peculiarity was the formation of cationic vacancies, as evidenced by the intense Raman band at 880–920 cm^{-1}, especially in samples with very low (Cr + V)/Sb ratio (i.e., a large excess of Sb) but higher relative amounts of V (e.g., a Cr/V ratio close to 1). In agreement with literature reports [39], this band is attributable to Sb–O–V stretching involving 2-coordinated O atoms adjacent to the cationic vacancies. This indicates the ability of the rutile compound to host excess Sb in the form of Sb^{5+}, with a corresponding generation of vacancies to compensate for the excess positive charge introduced in the structure. The intensity of this band can be correlated with the concentration of vacancies [41].

In the V/Sb/O, the nonstoichiometry originates from the existence of stable valence states higher than 3+ for V, with formation of mixed oxides in which the V^{4+}/V^{3+} ratio determines the amount of cationic vacancies while the overall V/Sb ratio remains close to 1 [41–44]. In some cases, in contrast, the overall V/Sb ratio may become >1; no cationic vacancies develop, because the V^{3+}/Sb^{5+} ratio remains equal to 1, and the presence of additional V^{4+} species is compensated for by the required amount of O^{2-} ions [45]. In rutile-type $CrSbO_4$, nonstoichiometry develops when Cr/Sb ratios <1 are used, with accommodation of excess Sb in the structure; this causes a decrease in crystallinity of the rutile [31].

The data obtained with Cr/V/Sb/Nb/O samples confirm indications formerly obtained with Nb-free catalysts. In general, samples with a large excess of Sb with respect to the (Cr + V) sum were less crystalline than those with an atomic (Cr+V)/Sb ratio closer to that required for stoichiometric rutile formation. The same samples were also those with the most intense band at 880–920 cm^{-1}. Excess Sb accommodated inside the rutile framework in the form of Sb^{5+}, replacing metal cations of lower charge; in such a way, cationic vacancies were generated.

The high intensity of the band at 880–920 cm^{-1} was also evident in those samples that, even with a relatively low Sb content, had a sufficient Nb content to develop a (Cr + V)/(Sb + Nb) atomic ratio <1. This provides an indication that Nb^{5+} replaced Sb in the rutile lattice, and that a mixed antimonate/niobate of Cr/V developed. Other indications supporting this hypothesis were (i) the presence of a single crystalline phase, but with a progressive shift of the X-ray reflections with increasing Sb content, and (ii) the modification of those Raman bands attributable to vibrations in the rutile structure. Specifically, a progressive increase of Sb led to a modification of features in the Raman spectrum from those typical of $CrNbO_4$ toward those of $CrSbO_4$, but with additional bands not typical of either of the two compounds. To the best of our knowledge, rutile-type compounds containing the four elements Cr, V, Sb, and Nb have not yet been described in the literature. In this compound, Nb^{5+} replaces both V and Sb^{5+}, causing an increased concentration of cationic vacancies and the segregation of antimony oxide, with an increased surface concentration of Sb^{3+}.

Our results also support an important role for vanadium. In those samples with lower V content, segregation of Sb oxide occurred in the presence of a large excess of Sb, whereas in the presence of increased amounts of low-valent V and Cr cations (e.g., in the Cr/V/Sb/Nb $1/1/x/1$ series), the rutile had a greater amount of Sb, in large excess with respect to the stoichiometric requirements, with no segregation of Sb oxide (see, e.g., the Raman spectra of Cr/V/Sb/Nb 1/1/3/1 and 1/1/5/1).

Therefore, the data indicate that one compositional parameter affecting the rutile characteristics is the (Cr + V)/(Sb + Nb) atomic ratio. When this ratio is between 0.5 and 1–1.2, the rutile-type mixed oxide was well crystallized, and the Raman spectrum was similar to that of Cr/V/Sb samples with a (Cr + V)/Sb ratio $\leqslant 1$. When the (Cr + V)/(Sb + Nb) ratio

is <0.5, due to the large excess Sb, the crystallinity was lower and the Raman spectrum was similar to that of Cr/V/Sb samples with a low (Cr + V)/Sb ratio.

Another important point concerns the negative effect of small amounts of crystalline or amorphous V_2O_5 on catalytic performance. In those samples in which V_2O_5 was present, most of the ammonia was burnt to N_2, and, correspondingly, the selectivity to products of partial ammoxidation was very low. Bulk vanadium oxide formed in samples with the higher V/(Sb + Nb) ratios. Crystalline V_2O_5 formed in those catalysts with the highest V content, such as Cr/V/Sb/Nb 1/1/0/1 and 1/1/1/1, as inferred from XRD patterns. However, small amounts of vanadium oxide were also found by Raman spectroscopy in samples with low V content but V/(Sb+Nb) atomic ratio ⩾0.2 (e.g., Cr/V/Sb/Nb 1/0.2/0/1 and 1/0.3/1.1/0).

Concerning the reason why Nb has a positive effect on the catalytic performance in propane ammoxidation to acrylonitrile, literature reports indicate that the development of crystalline $SbNbO_4$ lowers the activity [29,30]. In our case, additing Nb caused a decrease in activity only in samples with lower Sb content (Cr/V/Sb/Nb 1/0.2/1/x series), whereas the effect on activity was positive (albeit very low) in samples with higher Sb content. Mimura et al. [28] proposed the formation of $SbNb_{1-x}V_xO_4$ compound (with $x < 0.2$), in which the replacement of V^{4+} for Nb^{5+} led to the oxidation of Sb^{3+} (the species in stoichiometric $SbNbO_4$) to Sb^{5+}. In contrast, Bañares et al. [29,30] attributed the positive effect of Nb in V/Sb/Nb/O systems on selectivity to either the formation of sites with higher acid strength or a dopant effect on the catalytic properties of V/Sb/O. In rutile antimonates, it is well known that the major role in providing a high selectivity to acrylonitrile in propane ammoxidation is played either by the Sb oxide spread over the rutile surface [2,39,46–49] or by the incorporation of excess Sb in the outer atomic layers of rutile crystallites, as in Cr/V/Sb mixed oxides [31,33]. For our samples, the data suggest that this element does not play a direct role in allylic ammoxidation, but does improve the performance of Sb in this step. The most likely hypothesis for this effect is a modification of the properties of Sb sites at the surface of rutile crystallites, with generation of species with improved catalytic properties in allylic ammoxidation.

Cationic vacancies play an important role in the catalytic performance of rutile-type mixed oxides [41,44,50–53]. For instance, it was found that an increase in the concentrations of cationic vacancies and of isolated V^{4+} species in V/Sb/O systems due to introduction of increasing amounts of Fe in the lattice led to a proportionally higher activity [51]. The formation of V^{4+} in Cr/V/Sb mixed oxides had an analogous effect of a considerable increase in propane conversion [33,34].

In our samples, we found a progressively higher concentration of cationic vacancies, as inferred from the intensity of the band at 880–920 cm^{-1} in Raman spectra observed for the Cr/V/Sb/Nb 1/1/x/1 and 1/0.2/x/1 series, for increasing Sb content. However, the increase of cationic vacancies did not lead to a higher activity; on the contrary, the activity decreased. This can be explained by the fact, reported previously [42], that the introduction of excess Sb^{5+} in the rutile lattice led not only to an increase in the cationic vacancies, but also to a decrease in the V^{4+}content, which may be hypothesized to be a key to the activity. In contrast, an increase in Sb concentration led to considerably improved selectivity to acrylonitrile; hence, cationic vacancies might play a role in favoring the formation of this product.

The effect of Nb^{5+} on vacancy concentrations and V^{4+} content in the rutile phase and consequently on activity was less evident than that of Sb. One important effect of Nb addition was the increase in extrarutile Sb oxide, which is known to play an important and positive role in the selective formation of acrylonitrile [3,8,51]. But this cannot be the only reason for the improved selectivity. In fact, an increase in dispersed Sb oxide in the Nb-free samples led to better selectivity, albeit still lower than that achieved in the Nb-containing samples described in the present work. Also in this case, cationic vacancies may play an additional role in selectivity; their concentration also increased when the amount of Nb was increased. The neighboring of vacancies by Nb cations rather than Sb cations may generate sites in the rutile phase specific for the selective activation of ammonia and the generation of –N=H species. This implies a higher rate for the transformation of the unsaturated intermediate to acrylonitrile rather than to CO_2, and hence a greater selectivity with respect to converted ammonia, because the ammoxidation is in competition with the parallel reaction leading to the formation of N_2.

Catalysts containing Nb amounts comparable to those of Sb and a (Cr + V)/(Nb + Sb) ratio <1 were not tested; however, large amounts of Nb would be expected to cause the formation of relevant amounts of Nb oxide or of metal niobates (Cr/Nb/O and V/Nb/O). Tests on V/Nb/O have demonstrated that the rutile-type $VNbO_4$ is not stable in the reaction environment under hydrocarbon-lean conditions [38,54]. The structural stability of the catalyst in rutile-type Cr/V/Sb/Nb mixed oxides is provided by the presence of Cr and Sb, and thus by the formation of a Cr-based rutile-type antimonate, stable under the conditions for propane ammoxidation and inside which Nb dissolves with formation of the mixed antimonate/niobate. Vanadium also plays an important role, contributing to the improved catalytic activity; however, Cr/V ratios >1 are preferred, to avoid the formation of V_2O_5 and of V niobates and to limit the formation of propylene [33,34].

5. Conclusion

Adding Nb to rutile-type Cr/V/Sb mixed oxides led to a considerable improvement in the catalytic performance of propane ammoxidation to acrylonitrile. Specifically, a higher selectivity to acrylonitrile (up to 12% greater) and a small increase in propane conversion were obtained, with a corresponding remarkably lower combustion of ammonia to N_2. For Nb to have a positive effect on the catalytic performance of Cr/V/Sb/Nb mixed oxides, the following composition is required:

(a) A (Cr + V)/Sb ratio largely <1; this is related to the need for excess Sb to develop a Sb-enriched rutile mixed antimonate/niobate of Cr and V.

(b) A Nb/Sb ratio largely <1 but >0.05–0.1 (e.g., equal to 0.2–0.3); low amounts of Nb have a negligible effect on catalytic performance.

The positive effect of Nb was attributed to the formation of defective multicomponent rutile mixed oxides, containing the four elements in the same structure. These systems were also characterized by Sb^{5+} enrichment with respect to the stoichiometric composition, which provided efficient surface sites for allylic ammoxidation of the unsaturated intermediate. The data that we obtained in this study indicate that the concomitant presence of Nb and Sb in the rutile structure improved the efficiency of sites devoted to the insertion of activated ammonia, with a decrease in the rate of ammonia transformation to molecular nitrogen.

Acknowledgment

The authors thank Snamprogetti S.p.A. for financial support.

References

[1] Y. Moro-oka, W. Ueda, Catalysis, vol. 11, Royal Soc. Chem., London, 1994, p. 223.
[2] R.K. Grasselli, in: G. Ertl, H. Knözinger, J. Weitkamp (Eds.), in: Handbook of Heterogeneous Catalysis, vol. 5, Wiley–VCH, Weinheim, 1997, p. 2302.
[3] F. Cavani, F. Trifirò, in: M. Baerns (Ed.), Basic Principles in Applied Catalysis, in: Series in Chemical Physics, vol. 75, Springer, Berlin, 2003, p. 2.
[4] A.T. Guttmann, R.K. Grasselli, J.F. Brazdil, US Patent 4,788,317 (1988), to BP Amoco.
[5] T. Ushikubo, K. Oshima, T. Ihara, H. Amatsu, US Patent 5,534,650 (1996), to Mitsubishi Chem. Co.
[6] G. Centi, R.K. Grasselli, F. Trifirò, Catal. Today 13 (1992) 661.
[7] G. Blanchard, P. Burattin, F. Cavani, S. Masetti, F. Trifirò, WO Patent 97/23,287 A1 (1997), assigned to Rhodia.
[8] G. Centi, S. Perathoner, F. Trifirò, Appl. Catal. A: Gen. 157 (1997) 143.
[9] A. Andersson, S.L.T. Andersson, G. Centi, R.K. Grasselli, M. Sanati, F. Trifirò, in: L. Guczi, et al. (Eds.), New Frontiers in Catalysis, Elsevier Science, Amsterdam, 1993, p. 691.
[10] M.O. Guerrero-Perez, J.L.G. Fierro, M.A. Vicente, M.A. Bañares, J. Catal. 206 (2002) 339.
[11] T. Ushikubo, K. Oshima, A. Kayou, M. Vaarkamp, M. Hatano, J. Catal. 169 (1997) 394.
[12] M.O. Guerrero-Perez, J.N. Al-Saeedi, V.V. Guliants, M.A. Bañares, Appl. Catal. A: Gen. 260 (2004) 93.
[13] H. Watanabe, Y. Koyasu, Appl. Catal. A: Gen. 194 (2000) 479.
[14] J.M.M. Millet, H. Roussel, A. Pigamo, J.L. Dubois, J.C. Jumas, Appl. Catal. A: Gen. 232 (2002) 77.
[15] I. Nowak, M. Ziolek, Chem. Rev. 99 (1999) 3603.
[16] I.E. Wachs, J.-M. Jehng, G. Deo, H. Hu, N. Arora, Catal. Today 28 (1996) 199.
[17] K. Tanabe, S. Okazaki, Appl. Catal. A: Gen. 133 (1995) 191.
[18] D. Vitry, Y. Morikawa, J.L. Dubois, W. Ueda, Appl. Catal. A: Gen. 251 (2003) 411.
[19] P. Botella, J.M. Lopez Nieto, B. Bolsona, A. Mifsud, F. Marquez, J. Catal. 209 (2002) 445.
[20] R.K. Grasselli, J.D. Burrington, D.J. Buttrey, P. DeSanto Jr., C.G. Lugmair, A.F. Volpe Jr., T. Weingand, Top. Catal. 23 (2003) 5.
[21] M. Baca, A. Pigamo, J.L. Dubois, J.M.M. Millet, Catal. Commun. 6 (2005) 215.
[22] E.M. Thorsteinson, T.P. Wilson, F.G. Young, P.H. Kasai, J. Catal. 52 (1978) 116.
[23] R. Burch, R. Swarnakar, Appl. Catal. 70 (1991) 129.
[24] K. Ruth, R. Burch, R. Kieffer, J. Catal. 175 (1998) 27.
[25] M. Roussel, M. Bouchard, E. Bordes-Richard, K. Karim, S. Al-Sayari, Catal. Today 99 (2005) 77.
[26] R. Catani, G. Centi, J. Chem. Soc., Chem. Commun. (1991) 1081.
[27] I. Matsuura, H. Oda, K. Oshida, Catal. Today 16 (1993) 547.
[28] Y. Mimura, K. Ohyachi, I. Matsuura, Science and Technology in Catalysis 1998, Kodansha, Tokyo, 1999, p. 69.
[29] M.O. Guerrero-Perez, J.L.G. Fierro, M.A. Bañares, Catal. Today 78 (2003) 387.
[30] M.O. Guerrero-Perez, J.L.G. Fierro, M.A. Bañares, Phys. Chem. Chem. Phys. 5 (2003) 4032.
[31] N. Ballarini, F. Cavani, C. Giunchi, S. Masetti, F. Trifirò, D. Ghisletti, U. Cornaro, R. Catani, Top. Catal. 15 (2–4) (2001) 111.
[32] N. Ballarini, R. Catani, F. Cavani, U. Cornaro, D. Ghisletti, R. Millini, B. Stocchi, F. Trifirò, Stud. Surf. Sci. Catal. 136 (2001) 135.
[33] N. Ballarini, F. Cavani, D. Ghisletti, R. Catani, U. Cornaro, Catal. Today 78 (2003) 237.
[34] N. Ballarini, F. Cavani, M. Cimini, F. Trifirò, R. Catani, U. Cornaro, D. Ghisletti, Appl. Catal. A: Gen. 251 (2003) 49.
[35] J.M.M. Millet, M. Baca, A. Pigamo, D. Vitry, W. Ueda, J.L. Dubois, Appl. Catal. A: Gen. 244 (2003) 359.
[36] C.J. Chen, M. Greenblatt, K. Ravindran Nair, J.V. Waszczak, J. Solid State Chem. 64 (1986) 81.
[37] N. Ballarini, G. Calestani, R. Catani, F. Cavani, U. Cornaro, C. Cortelli, M. Ferrari, Stud. Surf. Sci. Catal. 155 (2005) 81.
[38] N. Ballarini, F. Cavani, C. Cortelli, C. Giunchi, P. Nobili, F. Trifirò, R. Catani, U. Cornaro, Catal. Today 78 (2003) 353.
[39] R. Nilsson, T. Lindblad, A. Andersson, J. Catal. 148 (1994) 501.
[40] C.A. Cody, L. Di Carlo, R.K. Darlington, Inorg. Chem. 18 (1979) 1572.
[41] M. Cimini, J.M.M. Millet, F. Cavani, J. Solid State Chem. 177 (2004) 1045.
[42] A. Landa-Canovas, J. Nilsson, S. Hansen, K. Ståhl, A. Andersson, J. Solid State Chem. 116 (1995) 369.
[43] T. Birchall, A.E. Sleight, Inorg. Chem. 15 (1976) 868.
[44] H. Roussel, B. Mehlomakulu, F. Belhadj, E. van Steen, J.M.M. Millet, J. Catal. 205 (2002) 97.
[45] F.J. Berry, M.E. Brett, W.R. Patterson, J. Chem. Soc. Dalton (1983) 9, 13.
[46] A. Andersson, S. Hansen, A. Wickman, Top. Catal. 15 (2001) 103.
[47] G. Centi, P. Mazzoli, Catal. Today 28 (1996) 351.
[48] G. Centi, F. Marchi, S. Perathoner, Appl. Catal. A: Gen. 149 (1997) 225.
[49] M.O. Guerrero-Perez, M.A. Bañares, Catal. Today 96 (2004) 265.
[50] M. Cimini, J.M.M. Millet, N. Ballarini, F. Cavani, C. Ciardelli, C. Ferrari, Catal. Today 91 (2004) 259.
[51] D.L. Nguyen, Y. Ben Taarit, J.M.M. Millet, Catal. Lett. 90 (2003) 65.
[52] J.M.M. Millet, J.C. Marcu, J.M. Herrmann, J. Mol. Catal. A: Chem. 226 (2005) 111.
[53] G. Xiong, V.S. Sullivan, P.C. Stair, G.W. Zajac, S.S. Trail, J.A. Kaduk, J.T. Golab, J.F. Brazdil, J. Catal. 230 (2005) 317.
[54] F. Cavani, N. Ballarini, M. Cimini, F. Trifirò, M.A. Bañares, M.O. Guerrero-Perez, Catal. Today 112 (2006) 12.